Optical Materials 95 (2019) 109219

Contents lists available at ScienceDirect

Optical Materials

journal homepage: www.elsevier.com/locate/optmat

Deposition of Rhodamine B dye on flexible substrates for flexible organic electronic and optoelectronic: Optical spectroscopy by Kramers-Kronig analysis

A.A.A. Darwish[a,b], A.M. Aboraia[c,d,*], Alexander V. Soldatov[c], I.S. Yahia[e,f,g]

[a] Nanotechnology Research Laboratory, Department of Physics, Faculty of Science, University of Tabuk, Tabuk, Saudi Arabia
[b] Department of Physics, Faculty of Education at Al-Mahweet, Sana'a University, Al-Mahweet, Yemen
[c] The Smart Materials Research Institute, Southern Federal University, Sladkova str. 178/24, Rostov-on-Don, Russia
[d] Department of Physics, Faculty of Science, Al-Azhar University, Assiut, 71542, Egypt
[e] Research Center for Advanced Materials Science (RCAMS), King Khalid University, Abha, 61413, P.O. Box 9004, Saudi Arabia
[f] Advanced Functional Materials & Optoelectronic Laboratory (AFMOL), Department of Physics, Faculty of Science, King Khalid University, P.O. Box 9004, Abha, Saudi Arabia
[g] Nanoscience Laboratory for Environmental and Bio-Medical Applications (NLEBA), Semiconductor Lab., Physics Department, Faculty of Education, Ain Shams University, Roxy, 11757, Cairo, Egypt

ARTICLE INFO

Keywords:
Kramers-Kronig
Rhodamine B dye
Flexible organic electronic
Linear/and nonlinear optics

ABSTRACT

Rhodamine B (RhB) films prepared via spin coater on polyacetate flexible substrates. The X-ray diffraction spectroscopy has been done for RhB/polyacetate flexible substrate and displays an amorphous structure of RhB films in the various thicknesses in the range of 74–303 nm. K-K relations used for determining the refractive index and exhibits a normal dispersion at $\lambda > 600$ nm and an anomalous dispersion at $\lambda < 600$ nm. The electronic transitions reveal two bands of absorbance Q band which due to the first $\pi\rightarrow\pi^*$ transitions and Soret band due to the second $\pi\rightarrow\pi^*$ transitions. Also, other linear optical constant such as absorption coefficient, band energy gap, dielectric constants, and optical conductivity were discussed. On the other hand, the first ($\chi^{(1)}$) and third ($\chi^{(3)}$) orders of nonlinear optical susceptibilities as well as a nonlinear refractive index (n_2) were calculated and discussed. The electrical and optical conductivities demonstrated the high absorption of RhB/flexible substrates inferring the chance of utilizing these films as optoelectronic gadgets.

1. Introduction

The advancement of flexible optoelectronic utilizing a flexible optically transparent substrate material and organic semiconductor materials has been generally used by electronic manufacture while creating new technological productions. The increasing interest in the advancement of flexible optoelectronic materials focuses on the continuous development of large-scale electronics as well as solar energy and biomedicine [1–3].

Organic laser dyes have been connected in the production of organic photovoltaics (OPVs) or dye-sensitized solar cells (DSSC). These dyes have a higher molar absorption coefficient contrasted with traditional dyes [4]. The one of a kind property of organic laser dyes offers access to an assortment of utilization in spectroscopy, optics, and lasers [5,6]. Rhodamine B (RhB) is one of significant laser dye with unique photophysical properties, for example, long wavelength emission on or absorption, large extinction coefficient, and high fluorescence quantum yield [4]. These properties make this dye valuable for an extensive assortment of uses, for example, electrochemical luminescence sensitizers, optical chemical sensors, solar collectors and biological stains [7–10].

Rhodamine dyes have several derivatives, for instance, RhB, Rhodamine 6G and Rhodamine 123 are in type dyes which emit red light through wavelength 600 nm. So, This type of dye suitable for biological application owing to the noninvasive nature of red light in the biological system [10]. RhB has optical properties in the liquid and solid state, for example, in liquid, the refractive index for RhB reaches ~1.35. The refractive index follows a non-linear increment for low doping wt% of RhB, while a linear increasing trend is seen at high doping wt% reaching almost constant values at higher doping [11].

* Corresponding author. The Smart Materials Research Institute, Southern Federal University, Sladkova str. 178/24, Rostov-on-Don, Russia. Tel.: +7 863 219 97 24 / +7 863 218 40 00.
E-mail addresses: a.m.aboraia@gmail.com (A.M. Aboraia), isyahia@gmail.com, ihussein@kku.edu.sa (I.S. Yahia).

https://doi.org/10.1016/j.optmat.2019.109219
Received 20 March 2019; Received in revised form 17 May 2019; Accepted 20 June 2019
0925-3467/

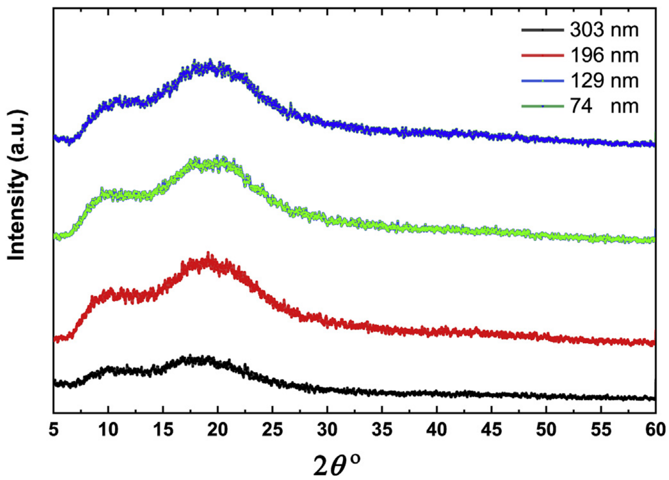

Fig. 1. XRD of RhB films deposited on a polyacetate flexible substrate.

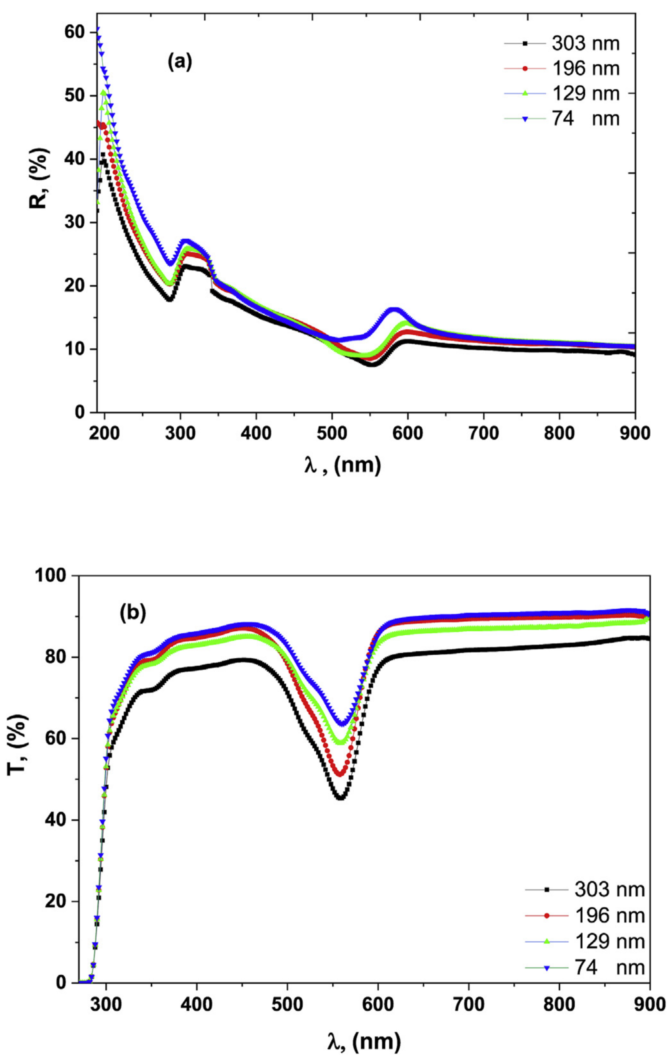

Fig. 2. (a,b): The spectral distribution of RhB films deposited on a polyacetate flexible substrate for (a) reflectance *R%* and (b) transmission *T%*.

RhB thin film was deposited by the drop casting technique, which has an amorphous structure and an optical band gap of 1.97 eV [12]. The impact of the thickness of RhB film on the electronic properties of the RhB/p-Si structure has been studied. It was found that interface state density diminishes with the lessening in film thickness [13]. A

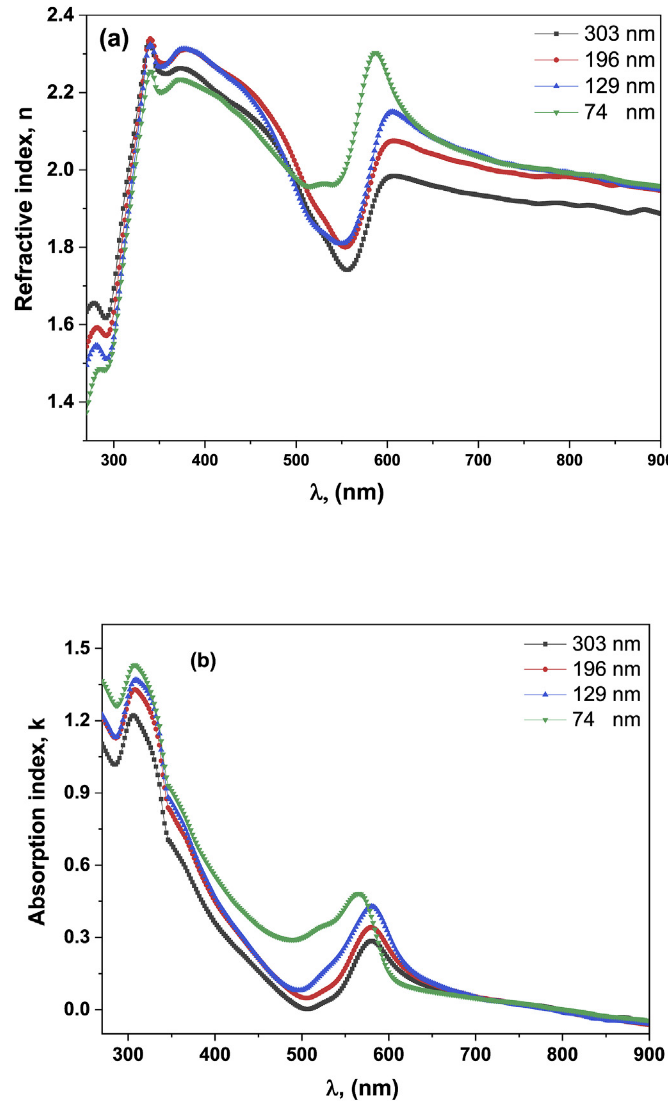

Fig. 3. (a,b): The spectral distribution of RhB films deposited on a polyacetate flexible substrate for: (a) refractive index (n) and (b) extinction coefficient (k).

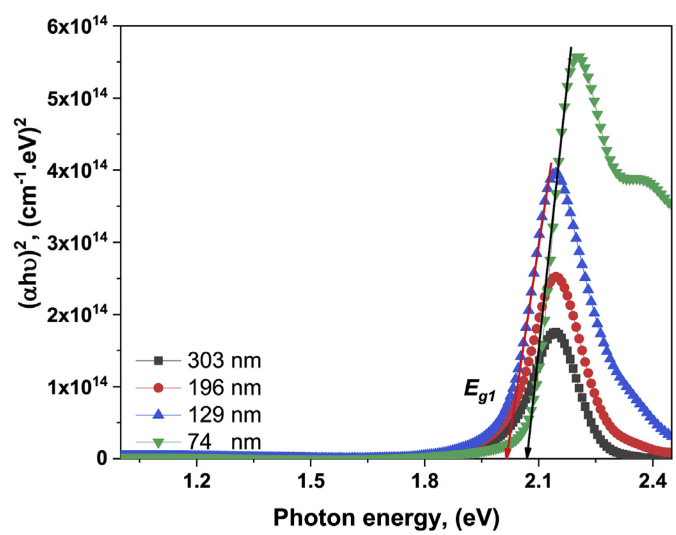

Fig. 4. The energy band gap of RhB films deposited on a polyacetate flexible substrate.

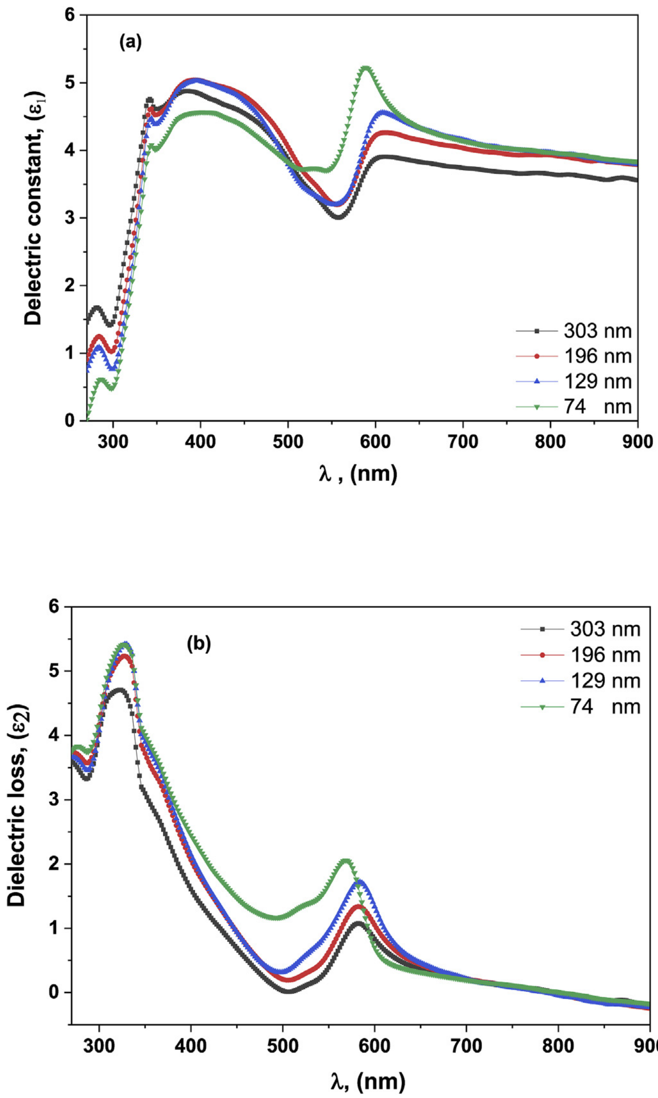

Fig. 5. (a,b): The spectral distribution of RhB films deposited on a polyacetate flexible substrate for (a) Real dielectric constant (ε_1) and (b) Imaginary dielectric constant (ε_2).

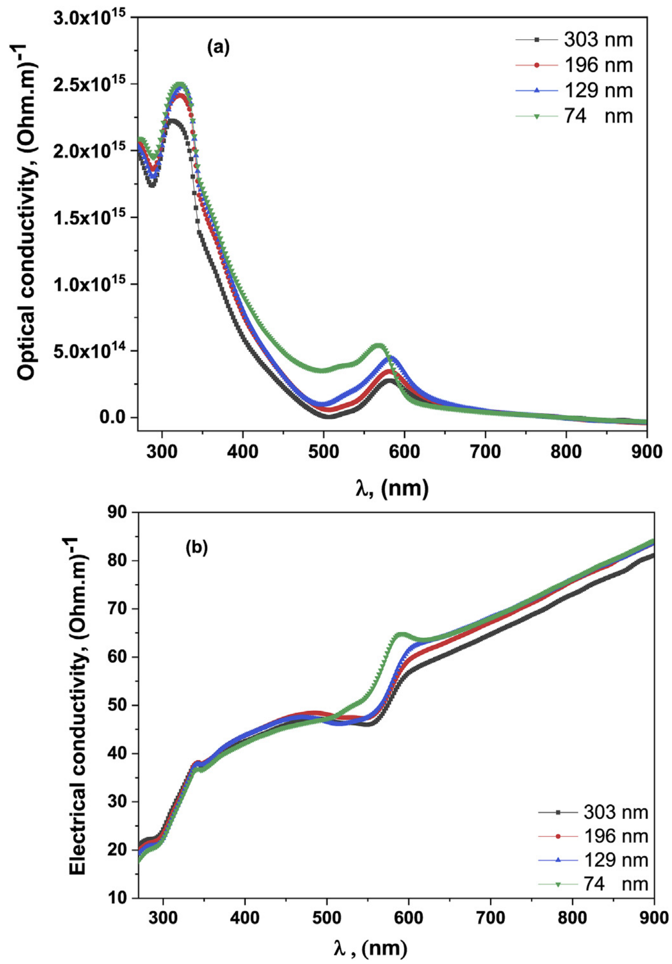

Fig. 6. (a,b): The spectral behaviors of (a) optical conductivity and (b) electrical conductivities for RhB films deposited on a polyacetate flexible substrate.

decent quality film of RhB on FTO substrate has been effectively accomplished by the spin coating method [14], and the linear and nonlinear optical constants were determined. These RhB films demonstrate the large nonlinear optical susceptibility when contrasted with other organic dyes [14]. Adding RhB laser dye as co-sensitizer in bulk heterojunction polymer solar cells was studied. The outcomes propose that RhB can be considered as an active material for application in polymer solar cells to achieve high photovoltaic execution [15].

The film thickness is essential parameters that can impact the structure and physical properties of films [16]. The impact of film thickness is required to adjust the homogeneity of films as the layers of the precipitation material is growing up, which in turns will diminish the deformities inside the films [17]. Additionally, the expansion in film thickness assumes a fundamental job in the agglomeration of stacking particles and hence will advance the growth of sublevel states number [17]. These logical reasons are adequate to modify the optical and electrical properties of the materials.

However, up to our knowledge, there is no revealed information about the RhB and their application in the field of electronics and optoelectronics. Films of RhB with different thicknesses were made on a polymer substrate by a spin coater technique. In this article, the Kramers-Kronig (*K-K*) method is utilized to figure the optical constants of RhB films by UV–Vis spectroscopy data [18,19]. The linear and nonlinear optical constants were calculated and discussed.

2. Experimental techniques

2.1. Synthesis of methyl violet-10B/FTO thin films

Rhodamine B (RhB) is an organic dye that can be used extensively as a tracer in water, biotechnology, fluorescence dye. The chemical formula of RhB is $C_{28}H_{31}ClN_2O_3$. RhB was used without any purification. 10-2 M of RhB powder was soluble in absolute ethanol for 20 min on a magnetic stirrer at 500 rpm at room temperature. After that, the soluble RhB was filtered to remove any residuals and keep in the dark desk for 24 h to avoid any light interaction with lights. Spin coating system was used to deposit the RhB on flexible polymeric substrates called poly (acetate) sheets as a highly transparent substrate. The thickness was varied with the changing of the speed of the rotation of the system at a constant time = 60 s. No, any post-annealing process was done on the studied samples.

2.2. Devices and measurements

The XRD patterns of RhB/Flexible substrates was measured using Shimadzu Lab X XRD-6000. This system was operated at 30 kV and 30 mA. The target inside the device is CuK_α monochromatic radiation.

The optical parameters such as absorbance *abs*(λ), transmittance *T*(λ), and reflectance *R*(λ) were scanned at various wavelengths from 285 to 2500 nm (i.e. UV–Vis–NIR regions) using JASCO

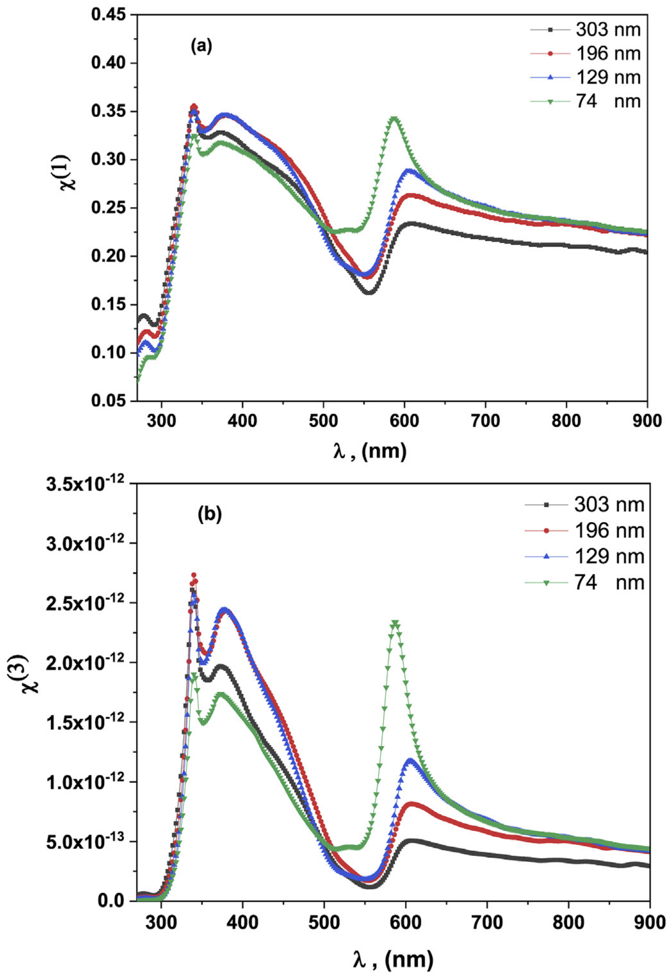

Fig. 7. (a,b): The spectral distribution of (a) linear optical susceptibility $\chi^{(1)}$ and (b) Nonlinear optical susceptibility $\chi^{(3)}$ for RhB films deposited on a polyacetate flexible substrate.

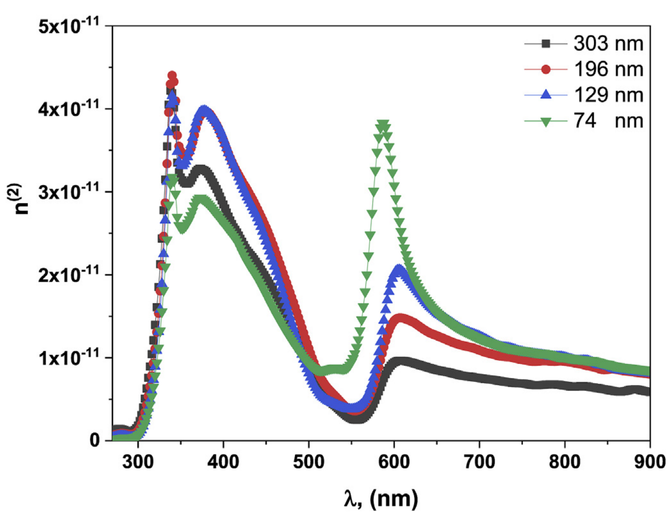

Fig. 8. The spectral distribution of n_2 for RhB films deposited on a polyacetate flexible substrate.

spectrophotometer, Model: V-570, at the normal incidence.

The laser power attenuation (i.e. optical limiting) of the two laser beams identified with wavelength as 632 and 533 nm were used. A homemade system with optical bench setup was used to measure the input/output of the incidents of laser beams on RhB/flexible poly (acetate) sheets.

2.3. Method of calculations

The *K-K* relation was utilized to figure the optical constants (*n* and *k*) of the RhB films from the reflectance measurements. The N' is presented by Ref. [20]:

$$N'(\omega) = n(\omega) + ik(\omega), \tag{1}$$

where ω is circular frequency, the n (ω) is the real part and the extinction coefficient k can be calculated based on the following equations:

$$n(\omega) = \frac{1 - R(\omega)}{1 + R(\omega) - 2\sqrt{R(\omega)}cos\varphi(\omega)}, \tag{2}$$

$$k(\omega) = \frac{1 - R(\omega)sin\varphi(\omega)}{1 + R(\omega) - 2\sqrt{R(\omega)}cos\varphi(\omega)}, \tag{3}$$

where the reflectance is R(ω) and u(ω) is the phase change at a specific wave number ω between the incidence and the reflected signal. This phase change calculated depend on K-K relation:

$$\varphi(\omega) = \frac{-\omega}{\pi}\int_0^\infty \frac{\ln R(\omega') - ln\, R(\omega)}{\omega'^2 - \omega^2}d\omega', \tag{4}$$

Eq. (4) can be portrayed as:

$$\Phi(\omega_j) = \frac{4\omega_j}{\pi} \times \Delta\,\omega \times \sum_i \frac{\ln(\sqrt{R(\omega)})}{\omega_i^2 - \omega_j^2}, \tag{5}$$

where $\Delta\omega = \omega_{i+1} + \omega_i$, and if the data interval j is an odd number, then *i = 2,4,6, ..., j-1, j + 1,...* while if *j* is an even number, then *i = 1, 3, 5, ..., j-1, j + 1,...*

3. Results and discussions

3.1. Structure analysis of RhB/polyacetate flexible substrate

The structure of RhB films deposited on a polyacetate flexible substrate of various thicknesses was broke down by utilizing the XRD strategy. The XRD of the RhB/polyacetate flexible substrate has appeared in Fig. 1. XRD curves display an amorphous structure of RhB films in the various thicknesses in the range of 74–303 nm.

3.2. Linear optical analysis of RhB/polyacetate flexible substrate

The spectral distribution of *R* and *T* of RhB films estimated in the wavelength run 190–900 nm appear in Fig. 2(a and b). Both the conduct of *R* and *T* respectively demonstrates the homogeneity and strength of the structure of RhB films as a result of the settlement of the position of the peaks in the absorbing area. Also, the spectral conduct of *T* for all thicknesses demonstrates an essential absorbance band at 550 nm. The nearness of such sharp band suggests these films are a decent filter material relying upon the wavelength. It could be noticed that all films turn out transparent at longer wavelengths (λ > 600 nm) and there are two edges of transmission. The complex refractive index was determined from *K-K* relations as notice above and Fig. 3 uncovers the dispersion of the refraction index (*n*) and extinction coefficient (*k*) of the RhB films against wavelength. The figure (Fig. 3a) of *n* indicates normal dispersion districts (λ > 600 nm). Likewise, the figure of *n* demonstrates anomalous dispersion (λ < 600 nm) and hence displays a multi-oscillator show in this range. The anomalous dispersion is because of the coupling of electrons in RhB films to the oscillating electric field excited because of the reverberation impact of the occurrence light and the electron polarization [21,22].

On the other hand, *k* (see Fig. 3b) diminished as the wavelength increments. The small estimations of *k* suggesting the deposited RhB film on a flexible substrate have an incredibly smooth surface [20]. The electronic transitions between orbits in the UV–Vis areas reveal two bands of absorbance, Soret, and *Q*-bands. The *Q*-band (500–650 nm) has been apportioned to the first π→π* transition. The band in the region of 250–350 nm (Soret band) could be a direct result of the second π→π* transition.

The most general model to examine the optical properties of semiconductor material is Tauc's model [23,24]. The band gap energy, E_g, can be obtained from the absorption coefficient, α, where $\alpha = 4\pi k/\lambda$. Tauc's model is used to determine the values of E_g for RhB films. The plot for the direct band gap appears in Fig. 4. The evaluation of direct E_g for the RhB films is dictated by extrapolating the straight parts of the curve of $(\alpha h\upsilon)^2$ versus $(h\upsilon)$ to the *x*-axis. The estimated Eg was around 1.95–1.98 eV and these values compatible with the value of the energy gap in Ref. [14].

The complex dielectric constant ($\varepsilon = \varepsilon_1 + i\ \varepsilon_2$) is a necessary amount which shed lights a more significant amount of clear insights regarding the collaborations among photons and electrons in a material. The real part, ε_1, called dielectric constant and the imaginary, ε_2, called dielectric loss. Fig. 5(a and b) demonstrates the spectra of ($\varepsilon_1 = n^2 - k^2$) and ($\varepsilon_2 = 2nk$) which they are called scattering and absorbance curves, separately. It is unmindful that the variety of ε_1 (Fig. 5a) demonstrates the same inclination from *n*, while the array of ε_2 (Fig. 5b) generally gives the same impression from *k* and the same behavior of ε_2 for FTO substrate with thickness 300 nm, on another hand in has different value for ε_1 may be attributed to the structure of substrate effect on the value of ε_1 [14]. The formation of tops in the dielectric spectra demonstrates different interactions delivered among photons and electrons in the films [25].

The optical conductivity ($\sigma_o = \alpha nc/4\pi$ where *c* is the speed of light) and electrical conductivity ($\sigma_e = 2\lambda\sigma_o/\alpha$) of various thickness RhB films were shown in (Fig. 6a) The optical conductivity has high value at sort wavelength demonstrates the high absorbance of RhB films. Additionally, (Fig. 6b) the electrical conductivity of contemporary films increases with expanding the wavelength. The high estimations of the optical and electrical conductivity of RhB films propose new applications in optoelectronic and photoelectric gadgets [26].

3.3. Nonlinear optical analysis of RhB/polyacetate flexible substrate

Films based on organic dyes have high nonlinear optical properties which give broad subtleties of the film and henceforth comprehension of how the light beams carry on through them [27]. The investigation of nonlinear conduct of the occurrence light assumes a vital job in the field of nonlinear optical gadgets, for example, optical switching gadgets, optical modulators, and optical signal processing [28]. In the present investigation, the first ($\chi^{(1)}$) and third ($\chi^{(3)}$) orders of nonlinear optical susceptibilities as well as a nonlinear refractive index (n_2) are assessed as published previously [4,14,23]. The equations can be summarized [4,14,23]:

$$\chi^{(1)} = (n^2 - 1)/4\pi, \tag{6}$$

$$\chi^{(3)} = A(\chi^{(1)})^4, \tag{7}$$

and

$$\chi^{(3)} = \frac{A}{(4\pi)^4}(n^2 - 1)^4, \tag{8}$$

$$n_2 = \frac{12\pi\chi^{(3)}}{n}, \tag{9}$$

Where *n* is the linear refractive index. Fig. 7(a and b) demonstrates the plots of $\chi^{(1)}$ and $\chi^{(3)}$ respectively, concerning the wavelength for the RhB films. The chart of $\chi^{(1)}$ unequivocally looks like that of ε_1 with a slight move in the wavelength demonstrating a sturdy reliance between them. The $\chi^{(1)}$ values are observed to be in the scope of 0.07–0.35. From this figure, both $\chi^{(1)}$ and $\chi^{(3)}$ pursue a comparative pattern in force variety against the wavelength for different thicknesses of RhB films. Fig. 8 depicts the plot of n_2 as for wavelength for the RhB films. It is a significant amount of the material which offers excellent information in regards to the light assembling limit of the film. The diagram precisely looks like that of $\chi^{(3)}$ and uncovers a substantial dependence of n_2 on $\chi^{(3)}$. It is clear for us from these results the behavior of nonlinear optical constant for flexible substrate have the same behavior for pyronin Y/flexible polymer, in contrast, the value of non-linear optical constant for FTO has different values may be attributed to the difference in the structure of substrate [14].

4. Conclusion

Films of Rhodamine B dye were prepared on flexible substrates to have an amorphous structure, which confirmed by X-ray diffraction spectroscopy. The Kramers-Kronig method was accustomed to getting the complex optical constants. The small estimations of extinction coefficient suggesting the deposited RhB film on a flexible substrate have an incredibly smooth surface. Tauc's model is used to determine the values of the energy band gaps for RhB films, which evaluated as direct energy band gaps. RhB films have one energy band was around 1.96 eV. RhB films/flexible substrate can be utilized in numerous applications, for example, electronic gadgets, flexible optoelectronic, and nonlinear optics with a predefined band gap.

Declaration of interests

There is no any conflict of interest.

Acknowledgment

The authors express their appreciation to "The Research Center for Advanced Materials Science (RCAMS)" at King Khalid University for funding this work under Grant Number (RCAMS-KKU/008-18).

References

[1] W.S. Wong, A. Salleo, W.S. Wong, A. Salleo (Eds.), Flexible Electronics: Materials and Applications, Springer, 2009.
[2] I.K. Popoola, M.A. Gondal, T.F. Qahtan, Renew. Sustain. Energy Rev. 82 (2018) 3127.
[3] J.H. Koo, J. Seo, T. Lee, Thin Solid Films 524 (2012) 1.
[4] M.M. Abutalib, I.S. Yahia, Optik 179 (2019) 145.
[5] D.S. Ahlawat, A.K. Sharma, L. Taneja, Rachna, R.D. Singh, Optic Commun. 282 (2009) 4256.
[6] Y. Jiao, L. Mao, S. Liu, T. Tan, D. Wang, D. Cao, B. Mi, Z. Gao, W. Huang, Dyes Pigments 158 (2018) 165.
[7] A. Silva, R.E.F. Boto, R.M. El-Shishtawy, P. Almeida, Eur. Polym. J. 42 (2006) 2270.
[8] T. Seckin, A. Gültek, S. Kartaca, Dyes Pigm. 56 (2003) 51.
[9] T. Ohishi, J. Non-Cryst. Solids 332 (2003) 80.
[10] Seyyed Mahdi Shavakandi, Khalil Alizadeh, Soheil Sharifi, Othmar Marti, Masoud Amirkhani, J. Phys. D Appl. Phys. 50 (2017) 155301.
[11] Jitendra Tripathi, Anupam Sharma, Shilpa Tripathi, Kallol Kumar Das, Macromol. Res. 24 (2016) 617–622.
[12] A.A.M. Farag, I.S. Yahia, Optic Commun. 283 (2010) 4310.
[13] M. Soylu, Mater. Sci. Semicond. Process. 14 (2011) 212.
[14] I.S. Yahia, Asim Jilani, M.M. Abutalib, S. AlFaify, M. Shkir, M.Sh Abdel-wahab, Attieh A. Al-Ghamdi, A.M. El-Naggar, Physica B 490 (2016) 25.
[15] S. Kazemifard, L. Naji, F.A. Taromi, J. Colloid Interface Sci. 515 (2018) 139.
[16] S.R. Alharbi, A.A.A. Darwish, S.E. Al Garni, H.I. ElSaeedy, K.F. Abd El-Rahman, Infrared Phys. Technol. 78 (2016) 77.
[17] H.M. Zeyada, M.M. EL-Nahass, S.A. Samak, J. Non-Crystal Solid 358 (2012) 915.
[18] J. Mobley, K.R. Waters, M.S. Hughes, C.S. Hall, J.N. Marsh, G.H. Brandenburger, J.G. Miller, J. Acoust. Soc. Am. 108 (2000) 2091.
[19] J.E. Nestell, R.W. Christy, Appl. Opt. 11 (1972) 643.
[20] S. Scheel, L. Knöll, D.G. Welsch, Phys. Rev. 60 (1999) 4094.
[21] M.M. Shehata, H. Kamal, H.M. Hasheme, M.M. El-Nahass, K. Abdelhady, Optic Laser. Technol. 106 (2018) 136.
[22] R. Al-Tuwirqi, A.A. Al-Ghamdi, N.A. Aal, A. Umar, W.E. Mahmoud, Superlattice. Microst. 49 (2011) 416.
[23] Mohammed A. Assiri, M. Aslam Manthrammel, A.M. Aboraia, I.S. Yahia, H.Y. Zahran, V. Ganesh, Mohd Shkir, S. AlFaify, Alexander V. Soldatov, Physica B 552 (2019) 62.

[24] F.S. Shokr, Optik 149 (2017) 270.
[25] M.M. El-Nahass, H.M. Abd El-Khalek, Ahmed M. Nawar, Opt. Commun. 285 (2012) 1872.
[26] P.A. Henikhena, Afr. Phys. Rev. 2 (2008) 68.
[27] M. Shkir, V. Ganesh, S. AlFaify, I.S. Yahia, J. Mater. Sci. Mater. Electron. 28 (2017) 10573.
[28] R. Swanepoel, J. Phys. E 17 (1984) 896.